MgH$_2$ Dehydrogenation Thermodynamics: Nanostructuring and Transition Metal Doping

S.A Shevlin,* Z. X. Guo

Department of Chemistry, University College London, Gower St, London, WC1E 6BT, United Kingdom

Abstract

Controversy currently exists as to the true effects of nanostructuring and transition-metal doping on the dehydrogenation of MgH$_2$. Following extensive datamining of structurally related compounds, we present for the first time, especially for the larger clusters, new stable structures for (MgH$_2$)$_n$ clusters, where n = 1 to 10. Using density functional theory and the harmonic approximation we determine the enthalpy of dehydrogenation for all of these clusters. All clusters have very different structures from the bulk, with one- to four-fold hydrogen coordinations observed, and three- to seven-fold magnesium coordinations. We find that, apart from the smallest clusters, enthalpy is larger than for the bulk. Nanostructuring does not improve dehydrogenation enthalpies. We attribute this to surface energy effects; as the (MgH$_2$)$_n$ clusters reduce in size bulk cuts become less stable until a stabilising reconstruction occurs which strongly modifies the cluster structure. This increases the magnitude of the dehydrogenation enthalpy. Accurately determining the structures of clusters is essential in determining gas-release thermodynamics for applications. Additionally we investigate modifications of these

clusters, in particular Ni-doping. We find that Ni substitutional doping energies are substantially lower than in the bulk, and that H_2 removal energies are substantially less. Nickel-doping will improve the dehydrogenation thermodynamics and kinetics of MgH_2 clusters.

Keywords: Hydrogen Storage, DFT modelling, nanostructuring, thermodynamics

1: Introduction

Energy storage and supply are urgent issues that need to be addressed by advanced societies for future prosperity. A transition needs to be made from the current energy economy, where fossil fuels dominate, to cleaner and renewable fuels. Hydrogen is a favoured replacement as it can be used as a fuel in combustion engines,[1] can be used in energy efficient fuel cells,[2] and has a large energy density of 119 kJ/mol. However the development of affordable, compact and safe storage and transportation systems for hydrogen presents real challenges.[2,3,4,5,6,7] A favoured material for hydrogen storage is magnesium hydride (MgH_2), as it has a high gravimetric hydrogen storage capacity of 7.6 wt% and is cheap and plentiful. However, unmodified MgH_2 is not suitable for technological applications due to a high enthalpy for dehydrogenation of 77 kJ/mol,[8] low plateau pressure of 10 Pa at ambient temperature and pressure,[9] and relatively slow absorption and desorption kinetics.[10]

Nanostructuring and doping are popular methods of modifying properties of materials, as is the case for MgH_2. Nanostructuring, via ball-milling,[11,12] or via wet-chemical synthesis using surface monolayer protection,[13,14,15] has being perceived to reduce the enthalpy for dehydrogenation. If H_2 release is a surface-desorption limited process,[16] then nanostructuring may modify surface curvature, hence dehydrogenation thermodynamics, and increase the specific surface area, hence dehydrogenation kinetics. Simulation has also demonstrated that nanoscale $(MgH_2)_n$ clusters, cut from the bulk, also possess lower dehydrogenation enthalpies than the bulk.[17,18,19,20] Interestingly however, in these simulations only very small clusters ($n = 1$ to 4) possess lower dehydrogenation

enthalpies than the bulk, larger clusters actually possess dehydrogenation enthalpies greater than that of the bulk, nanostructuring will only improve thermodynamic properties if it is possible to synthesize MgH_2 as molecular-size units, larger units are less stable than the bulk. At the nanoscale, it is well-known that cluster structures can be vastly different from the bulk, strongly modifying energetics. Furthermore, global structure determination is a major scientific problem.[21,22,23] As calculations on MgH_2 clusters use bulk cuts as starting structures there is a large degree of destabilisation, thus dehydrogenation enthalpies are underestimated. Previous work has only comprehensively searched the potential energy surface of the very smallest $(MgH_2)_n$ clusters, candidate global minima structures have not being demonstrated. Moreover, solid solutioning of other dopants, *e.g.* Ti, Fe and Ni, can also alter the electronic structure and bonding strength between hydrogen and Mg. Dopants that have been investigated include 3*d*-transition metals,[24,25,26] metal oxides,[27] and non-metallic elements, *e.g.* C and Si.[28,29,30] Among all the additives considered for modification of MgH_2 storage properties, Ni in particular shows great promise in reducing the dehydrogenation temperature and enhancing the hydrogen desorption kinetics. Liang *et al.* report that mechanically milled MgH_2 with Ni as a catalyst yields better absorption kinetics upon rehydrogenation than that of a mechanically alloyed Mg-Ni alloy.[24] However, catalysts do not substantially change the thermodynamic properties of MgH_2. It is an open question how nanostructuring affects the thermodynamics of doping.

In this Paper, we present the results of a systematic *ab initio* investigation of the geometry, electronic structure, and thermodynamics of the series of $(MgH_2)_n$ clusters, for

$n = 1$ to 10. We find, using initial structures datamined from the literature, several new structures for MgH_2 clusters that are significantly more stable than those previously reported. These structures are vastly different from the bulk cuts, with implications for the dehydrogenation enthalpy. The reconstruction of the $(MgH_2)_n$ clusters enhances stability, and for the majority of clusters surveyed increases the dehydrogenation enthalpy. Extrapolation to the bulk does not demonstrate any strong reduction in dehydrogenation enthalpy. We also demonstrate that transition metal doping, *via* nickel substitutional doping, is substantially easier for the clusters than for the bulk. This is due to the significantly enhanced surface energy. Nickel doping is, furthermore, demonstrated to be highly effective in modifying both dehydrogenation thermodynamics and kinetics.

2: Theory

The VASP density functional theory (DFT) program was used to model the structure and energetics of MgH_2 and Ni-doped MgH_2 systems.[31] DFT is the method of choice for both bulk and surface studies.[32] We consider both bulk MgH_2 and nanoscale $(MgH_2)_n$ particles, where $n = 1$ to 10. For all clusters, a cell of dimensions $15 \times 15 \times 15 \text{ Å}^3$ was used, energies are well converged for this unit cell size. A plane-wave cutoff of 370 eV was used for both undoped and doped cluster systems, with the Projector Augmented Wave method used to treat the core electrons.[33] In order to fully understand trends, all calculations were performed using several different exchange-correlation functionals, namely LDA,[34] PBE,[35] and PBESol.[36] Some additional calculations on the dehydrogenation enthalpy were performed using the B3LYP functional,[37,38] for these we only consider dehydrogenation from the $n = 2, 4, 6, 8$, and 10 clusters. We present the

results of our PBESol calculations, with LDA and PBE structures shown in the Supplementary Information. After complete dehydrogenation, the end-products are the clusters Mg_n, where $n = 1, 2, 3, 4, 5, 6, 7, 8, 9$, and 10. These clusters were also modelled, and taken to be global minima. [39] Temperature corrections to the internal energy are calculated within the harmonic approximation. All dehydrogenation enthalpies are calculated at a temperature of 573 K, to enable comparison with experiment. The enthalpy of the H_2 molecule is calculated by taking the zero-point energy and adding 5/2 kT.[40] From a simple thermodynamic analysis dehydrogenation enthalpies suitable for hydrogen release at room temperature are those between 0.31 and 0.62 eV/H_2.[4]

For each cluster n the thermodynamics of nickel-doping is also investigated, this involves the replacement of a single Mg atom with a single Ni atom. Dopant formation energies are calculated with respect to the bulk Mg and Ni crystals. All of these calculations were performed using the PBESol functional, as the PBESol functional was designed to improve the performance of GGA functionals in describing solids. It is therefore most likely to minimize errors when considering the combination of MgH_2, Mg, and Ni solids. Furthermore, all calculations were spin-polarised. Multiple Ni doping sites are considered for each cluster, we consider all possible Ni dopant sites for each cluster, e.g. three-fold, four-fold, five-fold, six-fold and seven-fold site. We thus performed twenty separate calculations in total. As there are no global minimum structures for Ni-doped Mg clusters, we cannot rigorously determine dehydrogenation enthalpies. In order to determine the effect of Ni-doping on hydrogen release properties, we calculate the hydrogen removal energy

$$E_{Rem} = E_{Tot}(Mg_nH_{2n}) - E_{Tot}(H_2) - E_{Tot}(Mg_nH_{2n-2})$$

where $E_{Tot}(Mg_nH_{2n})$ is the total energy of a $(MgH_2)_n$ cluster, $E_{Tot}(H_2)$ is the energy of an isolated hydrogen molecule in free space, and $E_{Tot}(Mg_nH_{2n-2})$ is the total energy of a $(MgH_2)_n$ cluster after 2H atoms are removed and the cluster is allowed to relax. The more positive E_{rem} the stronger the hydrogen is bound. For room temperature applications, removal energies from 0.2 to 0.7 eV/H_2 are desirable.[4] It is not known *a priori* which Mg_nH_{2n-2} cluster has the lowest energy structure, therefore we relaxed multiple Mg_nH_{2n-2} structures. Each structure was generated by removing two H atoms from the parent Mg_nH_{2n} cluster. For each cluster we exhaustively survey all potential hydrogen deficient clusters and take the lowest energy structure, this is done by removing all possible pairs of hydrogen atoms that are symmetry inequivalent (e.g., have different local bonding). In total, sixty-nine hydrogen-deficient clusters were considered. The same procedure is also used for the lowest energy Ni-doped clusters; where in total forty-two hydrogen-deficient clusters were considered.

To facilitate comparison of cluster thermodynamics and dopant energies with the bulk, simulations of MgH_2, Mg, and Ni were performed. A Monkhorst-Pack net was used to sample reciprocal space, with a net of (3×3×3) used for MgH_2, and (11×11×11) nets for Mg and Ni. Lattice parameters for MgH_2 were found to be $a = 4.460$ Å (underestimate of 0.9%), $c = 2.987$ Å (underestimate of 0.8%).[41] Lattice parameters as found with LDA, PBE and PBESol are shown in Supplementary Information. The numbers in brackets are

percentage underestimates when compared to experiment. For Mg we find lattice vectors of $a = 3.177$ Å (an underestimate of 1.0%) and $c = 5.152$ Å (an underestimate of 1.2% compared to experiment), while for Ni we find $a = 3.462$ Å, an underestimate of 1.6% compared to experiment. We determine the surface energies of MgH$_2$–(110) and Mg–(0001) (the lowest energy surfaces) with PBE, by using (2×2×3) supercells for MgH$_2$ and (3×3×5) supercells for Mg. Substitutional Ni doping of MgH$_2$ is modelled using a (4×4×5) unit cell, where one Ni atom substitutes for one Mg. All structures were relaxed until the change in energy was less than 10^{-7} eV, with all interatomic forces converged to 0.001 eV/Å. The stability of all structures was checked using vibrational analysis.

3: Results

3.1: Cluster structure determination and thermodynamics

Bulk cuts of MgH$_2$ will not be stable at the nanoscale, therefore we must seek alternative structures. We found candidate structures for (MgH$_2$)$_n$ clusters by datamining the literature of cluster structures of compounds with similar structures and stoichiometries. In particular, we use (TiO$_2$)$_n$ clusters as initial structures for relaxation, as TiO$_2$ has a stable phase with the rutile structure. There is a considerable amount of literature on the global minima structures of TiO$_2$ clusters.[22,42,43,44,45] Furthermore, in order to check the rigorousness of this approach we also considered candidate structures derived from different materials, namely SiO$_2$,[46] and MgF$_2$.[47,48] In order to survey the potential energy surface, especially of the smaller nanostructures, we relaxed many (59 in total) candidate structures. The lowest energy, and for certain sizes second lowest energy, cluster structures are shown in Figure 1. It is clear that the structural motifs present in these

clusters are significantly different from the bulk, where hydrogen is three-fold bound to magnesium, and magnesium is six-fold bound to hydrogen. In the clusters one- to three-fold hydrogen coordination can be seen, with four- to seven-fold magnesium coordination. From comparison of our results obtained with different functionals we see that different lowest energy structures are found with different functionals, see the Supplementary Information. We are able to compare the stability of our structures with those of Koukaras *et al.*,[20] and can report that apart from the smallest clusters our structures are more stable than those reported. Our cluster structures are more stable by 0.009 eV to 0.321 eV, with the PBE functional, 0.015 to 0.233 eV with the LDA functional, and 0.011 to 0.273 eV with the PBESol functional. In particular, we find much lower energies for the larger clusters, with major implications for extrapolation to the bulk. The lowest energy structures are typically those that were sourced from TiO_2, SiO_2-derived and MgF_2-derived structures are higher in energy.

For $(MgH_2)_2$, we find that a flat cluster structure composed of two slightly bent MgH_2 monomers forming a square is most preferred. It is feasible to generate larger linear cluster structures using this initial structure, e.g. for $(MgH_2)_3$ or $(MgH_2)_4$, but they are higher in energy than more compact structures. There are clear structural similarities between $(MgH_2)_3$, $(MgH_2)_4$, and $(MgH_2)_5$, with two one-fold hydrogens at either end of the cluster. All of these clusters have high degrees of symmetry, however $(MgH_2)_6$ and larger clusters do not. Indeed, $(MgH_2)_6$ has a strong resemblance to $(MgH_2)_5 + MgH_2$ bound together, but with additional distortion, and $(MgH_2)_7$ resembles $(MgH_2)_6 + MgH_2$ with additional distortion. The $(MgH_2)_8$ cluster has a very high degree of symmetry; we

therefore expect this cluster to be more stable towards dehydrogenation than other clusters of a similar size. Both $(MgH_2)_9$ and $(MgH_2)_{10}$ are more compact clusters with no short H-H distances. Both of these clusters feature (strongly distorted) MgH_6 octahedra, two for $(MgH_2)_9$ and six for $(MgH_2)_{10}$, and thus demonstrate some bulk-like structure. In general, as outlined in the Supplementary Information, the potential energy surfaces of MgH_2 clusters are quite similar for LDA, PBESol, and B3LYP functionals, all of which strongly differ with the PBE results. Additionally, we have compared our cluster structures to relaxations of bulk cuts, specifically $(MgH_2)_4$, $(MgH_2)_6$, and $(MgH_2)_{10}$, all of which are higher in energy (by 0.1180 eV/f.u., 0.1580 eV/f.u., and 0.0417 eV/f.u. respectively).
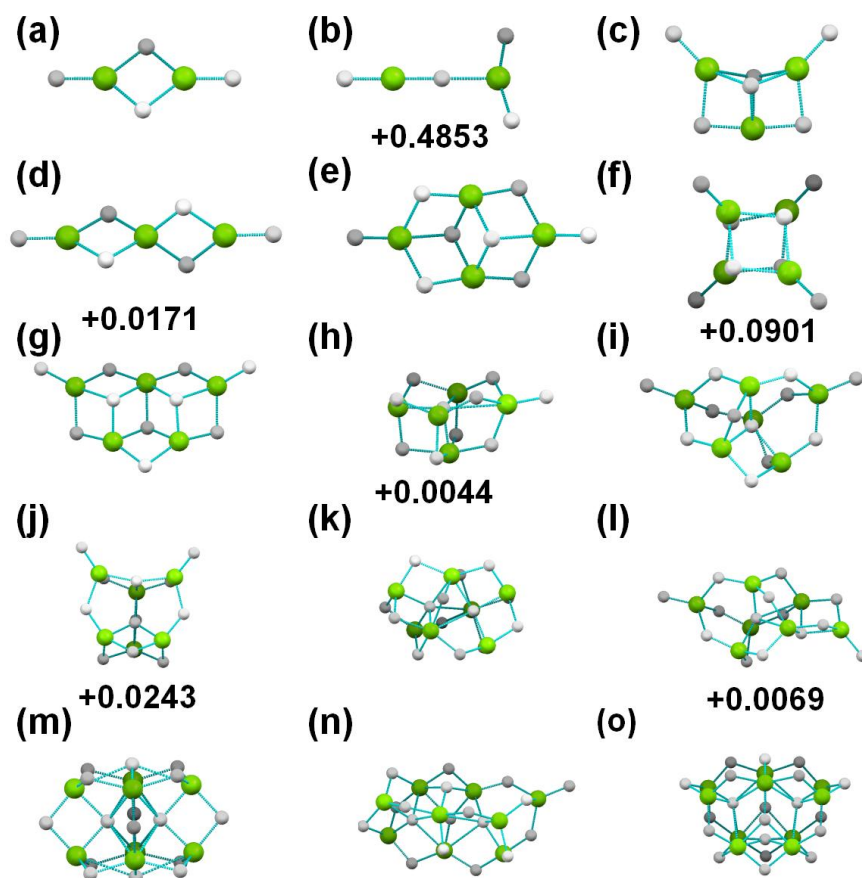
Figure 1: Minimum energy structures of $(MgH_2)_n$ clusters as found with the PBESol functional: (a) $n = 2$, (c) $n = 3$, (e) $n = 4$, (g) $n = 5$, (i) $n = 6$, (k) $n = 7$, (m) $n = 8$, (n) $n = 9$ and (o) $n = 10$. The second lowest clusters for $n = 2$ (b), $n = 3$ (d), $n = 4$ (f), $n = 5$ (h), $n = 6$ (j), and $n = 7$ (l) are also shown, the number below each of these structures is the total energy difference in eV per formula unit when compared to the lowest energy structures. Magnesium is represented by the green sphere, and hydrogen by the white spheres.

Using the lowest energy structures, the dehydrogenation thermodynamics for the cluster structures and the bulk were determined; see Figure 2, with values given in the Supplementary Information. We present results as calculated using all functionals. For the bulk, dehydrogenation enthalpies calculated using the LDA functional, at 0.851 eV/H_2, are closest to the experimental value for the dehydrogenation enthalpy of 0.805 eV eV/H_2 at 573 K, Ref 8. The PBE functional strongly underestimates the dehydrogenation enthalpy, with a value of 0.497 eV/H_2, an underestimate of 38%. The PBESol functional only partially corrects for this underestimate giving a value of 0.563 eV/H_2. Due to the well-known issues regarding hybrid functionals and metal systems, we do not calculate bulk dehydrogenation enthalpies with the B3LYP functional. Furthermore, it is apparent that dehydrogenation enthalpies are largest as found with the LDA and are smallest as found by the PBE. Both B3LYP and PBESol calculations find intermediate dehydrogenation enthalpies. Our results are in agreement with the conclusions of Pozzo *et al.*, who found that due to a fortuitous cancellation of errors the

LDA functional most accurately determines the dehydrogenation enthalpy of bulk MgH$_2$.[49]

For the LDA, PBE, and PBESol functionals we can explicitly compare nanoparticle dehydrogenation enthalpies to the bulk. Only the smallest cluster, the (MgH$_2$)$_2$ cluster has a smaller dehydrogenation enthalpy than the bulk as found by all three functionals. Using the PBE and PBESol functionals the (MgH$_2$)$_3$ and (MgH$_2$)$_4$ clusters have similar dehydrogenation enthalpies than the bulk, whereas with the LDA functional these clusters have slightly smaller dehydrogenation enthalpies. With all functionals larger clusters have larger dehydrogenation enthalpies than the bulk. We conclude that nanostructuring will not improve the thermodynamics for H$_2$ release, unless the (MgH$_2$)$_2$ cluster can be formed. With our comprehensive survey of cluster structures we have a strongly different energy profile for the clusters than that determined by Wagemanns *et al.*,[17] who found that nanostructuring MgH$_2$ improved dehydrogenation thermodynamics for $n = 2$ to 6. In comparison with Wu *et al.*, our PBE dehydrogenation enthalpies are higher for all clusters, while our LDA dehydrogenation enthalpies are lower for large clusters.[19] For the PBE case we attribute this difference to our choice of more stable structures for the clusters increasing the enthalpy of dehydrogenation. Furthermore, Wu *et al.* use a localised triple-ζ basis set which typically for larger clusters provide enhanced stability. Finally, we note that for smaller clusters ($n = 2$ to 5) our PBESol calculations are in agreement with the highly accurate quantum Monte Carlo calculations of Wu *et al.*, while for larger clusters ($n = 6$ to 10) our LDA calculations are in agreement with the quantum Monte Carlo calculations. For reference, the dehydrogenation enthalpies of several MgH$_2$

clusters were determined using the B3LYP functional. As for the quantum Monte Carlo calculations of Wu *et al.* the smaller cluster enthalpies are in closer agreement with PBESol results while larger cluster dehydrogenation enthalpies are in closer agreement with LDA results. The PBE enthalpies fare the worst in matching the hybrid functionals. This is somewhat counterintuitive, PBESol functionals are optimised for bulk systems therefore it would be expected that they would do worse for cluster systems than normal PBE. This is not the case here. For the size regime where nanostructuring is expected to have a neutral or beneficial effect on thermodynamics, the PBESol functional results should give the best agreement with experiment for non-hybrid functionals. We surmise that the self-interaction error of PBESol for MgH_2 clusters is reduced when compared with PBE. Indeed, our PBESol calculations strongly indicate that nanostructuring does not improve H_2-release thermodynamics with respect to the bulk, in agreement with experiment.[50] Our results are in agreement with the work of Reich *et al.*, who determined from simulation of a single amorphous $(MgH_2)_{31}$ cluster that nanostructuring does not improve dehydrogenation thermodynamics.[51] Unlike the work of Reich *et al.*, we have sampled many potential cluster structures and furthermore have considered different cluster sizes. We have demonstrated the existence of substantially more stable clusters at larger sizes. As MgH_2 cluster stability increases for a given cluster size, dehydrogenation enthalpy increases. Thus nanostructuring does not improve thermodynamics, only kinetics.

Finally, we can extrapolate from our enthalpies for dehydrogenation of MgH_2 clusters to the bulk, taking the values for $n = 6, 7, 8, 9,$ and 10 and fitting to a quadratic curve. We

find that both LDA and PBESol functionals predict that for infinite cluster size dehydrogenation enthalpies are lower than those predicted for the bulk, significantly so at 0.739 eV/H_2 for LDA and slightly smaller for PBESol 0.543 eV/H_2. In contrast, reinforcing our observation that the PBE functional is quantitatively different for MgH_2 than the LDA and PBESol functionals, we find at infinite cluster size dehydrogenation enthalpy is at 0.511 eV/H_2 greater than the predicted value for the bulk. Even for the best case scenario, dehydrogenation enthalpy is not strongly modified. Based on the variety of structures considered, extrapolation from low-energy cluster structures does not indicate that noncrystalline structures possess better dehydrogenation thermodynamics, in contradiction with previous suggestions.[20]

It has been predicted that due to surface energy effects, reducing the size of MgH_2 crystallites will result in a reduction of dehydrogenation enthalpy.[6,52] Furthermore, simulations on Mg nanowires of various diameters also find a direct dependence on nanowire diameter and desorption enthalpy.[53] As the surface energy of MgH_2(110) (0.43 Jm^{-2} in our calculations) is greater than the surface energy of Mg(0001) (0.32 Jm^{-2}), with decreasing particle size hydrogen desorption enthalpy decreases. This is due to the correction factor to the enthalpy of[6]

$$\Delta H = \Delta H^0 + 3\frac{V_{Mg}\gamma_{Mg}}{\gamma_{Mg}} - 3\frac{V_{MgH_2}\gamma_{MgH_2}}{\gamma_{MgH_2}}$$

where ΔH is the enthalpy of the cluster, ΔH^0 is the entropy of the bulk, V_{Mg} is the molar volume of magnesium and γ_{Mg} is the surface energy density of magnesium, while V_{MgH2} is the molar volume of MgH_2 and γ_{MgH2} is the surface energy density. The key difference between these analyses and our results is that the authors assume that the structures of the

Mg and MgH$_2$ crystallites remain bulk-like into the nanoscale. Our MgH$_2$ cluster structures, as outlined above, are radically different from the bulk. This is clearly caused by the increasing surface energy due to decreasing cluster size; at a critical size reconstruction of the bulk cuts will become energetically preferred, with an associated decrease in surface energy. In contrast, the Mg clusters do not strongly reconstruct. As the surface energy of the MgH$_2$ cluster is smaller than the surface energy of the corresponding Mg cluster, then the enthalpy of dehydrogenation will increase. In fact, this stabilisation effect upon large-scale reconstruction is a general result independent of material. Upon large-scale reconstruction of a cluster structure, simple trends extrapolated from the bulk are no longer valid.
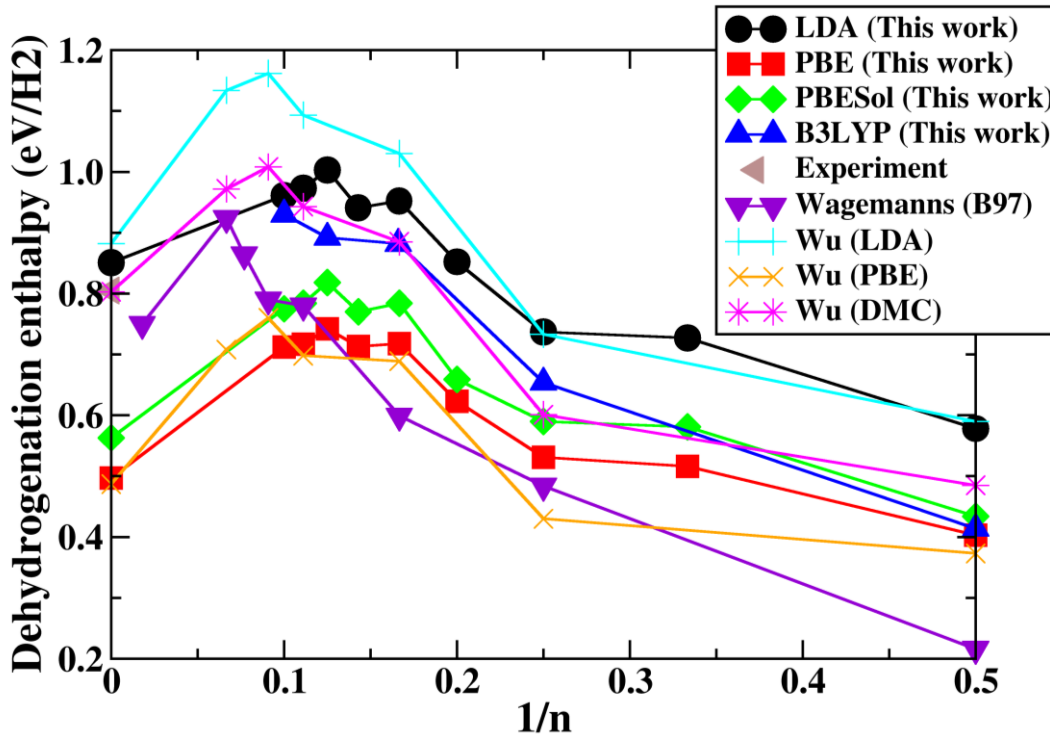

Figure 2: Dehydrogenation enthalpies per H$_2$ molecule for (MgH$_2$)$_n$ clusters, as obtained using various functionals, plotted as 1/n. For comparison we also show dehydrogenation enthalpies obtained from Wagemann *et al.* (ref 17) and Wu *et al.* (ref 19) for different

cluster sizes, and the experimental value for the bulk (ref **Error! Bookmark not defined.**). The functional used for each calculation, as well as the lead author, is identified in the inset, while DMC refers to a quantum Monte Carlo calculation.

3.2: Nickel doping

Experimentally, transition metal dopants have been shown to improve hydrogen storage thermodynamics. Substitutional doping of nickel onto magnesium sites of the MgH_2 crystal has been demonstrated to reduce dehydrogenation thermodynamics.[18,25] Interstitial doping sites for Ni dopants are lower in energy,[54] however upon complete dehydrogenation to Mg the Ni interstitials would migrate to fill Mg vacancies. As the $(MgH_2)_n$ clusters present radically different structural motifs to the bulk, it is expected that the defect formation energies are also different.

We performed a comprehensive survey of the Ni-dopant sites and energetics for $(MgH_2)_n$, where $n = 2$ to 10. The lowest energy site for each Ni dopant is shown in Figure 3. To simplify discussion, in this section we use $(MgH_2)_n$ to refer to a Ni-doped cluster, e.g. $(MgH_2)_5$ represents $(MgH_2)_4NiH_2$. As can be observed, the Nickel atom prefers to substitute for Mg atoms that bind to multiple hydrogen atoms. Furthermore, the Ni dopant has a strong perturbative effect on the hydrogen atoms surrounding it, shortening H-H bonds, in particular for $(MgH_2)_5$. The Ni–H bonds are significantly shorter than the Mg–H bonds, with he former being between 1.4 and 1.6 Å and the latter being between 1.9 and 2.1 Å.
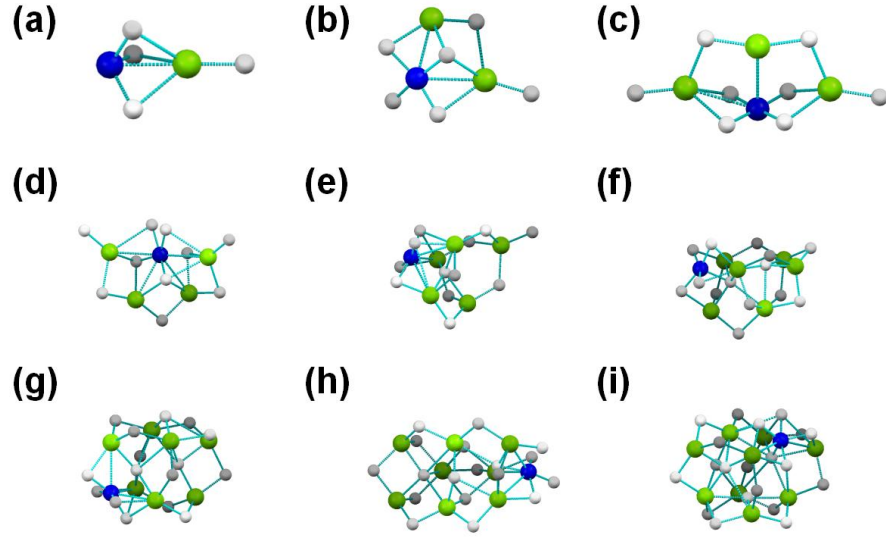
Figure 3: Lowest energy Ni doping sites, for $(MgH_2)_n$ clusters, where $n =$ (a) 2, (b) 3, (c) 4, (d) 5, (e) 6, (f) 7, (g) 8, (h) 9, and (i) 10. Blue spheres represent the Ni dopant.

The dopant formation energy is calculated using

$$E_F(Mg_{n-1}NiH_{2n}) = E_{Tot}(Mg_{n-1}NiH_{2n}) + E_{Tot}(Mg) - E_{Tot}(Mg_nH_{2n}) - E_{Tot}(Ni)$$

where $E_{Tot}(Mg_{n-1}XH_{2n})$ is the energy of the doped cluster, $E_{Tot}(Mg)$ is the energy of a Mg atom (using bulk Mg as the reference), $E_{Tot}(Mg_nH_{2n})$ is the energy of the undoped cluster, and $E_{Tot}(Ni)$ is the energy of a Ni atom (using bulk Ni as the reference). The defect formation energies are shown in Table 1. It is immediately obvious that for all of the clusters where $n \geq 3$ it is far easier to substitute Ni into the MgH_2 lattice than for the bulk. Indeed, for $n = 5, 6, 8,$ and 9 the energy cost is trivial, with the $(MgH_2)_8$ cluster unstable with respect to Ni-doping.

	E_F (eV)
Bulk Rutile MgH$_2$	1.64
(MgH$_2$)$_2$	2.01
(MgH$_2$)$_3$	0.60
(MgH$_2$)$_4$	0.22
(MgH$_2$)$_5$	0.01
(MgH$_2$)$_6$	0.00
(MgH$_2$)$_7$	0.21
(MgH$_2$)$_8$	-0.08
(MgH$_2$)$_9$	0.00
(MgH$_2$)$_{10}$	0.15

Table One: Calculated defect formation energies for Ni_{Mg}^X dopants. Units are in eV

As Ni dopants have a significant effect on the geometry and electronic structure of the MgH$_2$ cluster, we also calculated the effects on the dehydrogenation thermodynamics. In particular we calculate the removal energy for first H$_2$ removal from both the undoped and Ni-doped MgH$_2$ clusters, see Figure 4. As outlined in the Results section, we do not consider Ni-doped Mg clusters. Ni-doping significantly reduces the removal energy, typically by 0.2 to 0.6 eV. Similar results have been observed for Ti or Fe-doping of (MgH$_2$)$_{31}$, see Ref 43. In particular, Ni-doping has a significant effect on the (MgH$_2$)$_8$ and (MgH$_2$)$_{10}$ clusters, lowering their removal energies to 0.28 and 0.13 eV/H$_2$ respectively. This is in the ideal range for room-temperature hydrogen release. For ideal clusters, initial H-release involves the liberation of the weakly bound one-fold coordinated and two-fold coordinated hydrogens. However, for Ni-doped clusters initial hydrogen release is from a hydrogen atom of the NiH$_4$ complex and a neighbouring hydrogen which is not bound to the nickel atom.
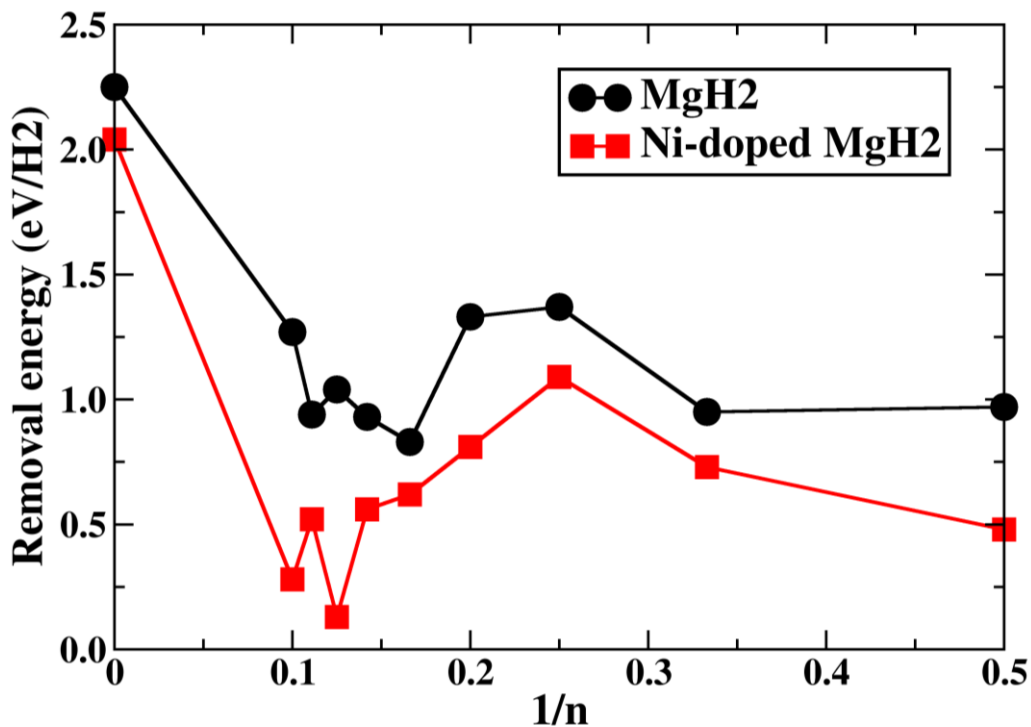
Figure 4: Calculated removal energies for single H_2 removal from undoped and Ni-doped $(MgH_2)_n$ clusters. All units are in eV.

We calculated the charge deformation density in order to understand the effects of Ni dopants on the electronic structure of the MgH_2 clusters and thus the mechanism behind the reduced removal energy, see Figure 5. There is significant electronic density donation from the H^- ions to an empty d-state of the Ni dopant. This can also be observed in Bader partial charge analysis, where in the undoped clusters the hydrogen has an average charge of $-0.78e$ but upon Ni-doping the four hydrogen atoms of the NiH_4 complex have a reduced charge of $-0.38e$. As the Mg–H bond is partially ionic, any reduction of the H^- anion charge will weaken the bonding between these ions, while as H^- cannot donate all of its electron density to the Ni dopant any Ni–H bonds formed will be weaker than in the

bulk. Hence the competition of these two effects acts to destabilise hydrogen bonding in the Ni-doped cluster.
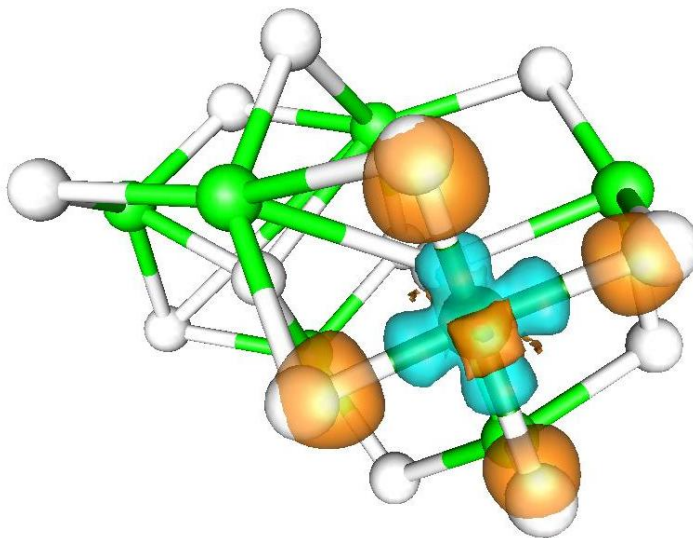

Figure 5: Charge density difference of Ni-doped $(MgH_2)_7$, orange denoting charge density depletion and blue denoting charge density accumulation. Electronic density is transferred from H^- ion to d-state of the Ni dopant. Isosurfaces are drawn at 0.1 $|e|Å^3$.

4: Conclusions

We have obtained the structural and thermodynamic properties a representative variety of $(MgH_2)_n$ clusters, where $n = 1$ to 10. We thus discover new low-energy structures, which possess radically different structural motifs than the bulk rutile phase, with hydrogen atoms forming single, double, triple, and quadruple bonds with magnesium. Using accurate calculations of the dehydrogenation enthalpy, we demonstrate that, considering our new low energy structures as strongly favoured in the nanostructuring process, nanostructuring at these sizes do not improve dehydrogenation thermodynamics. Indeed, nanostructuring provides a slight worsening of dehydrogenation thermodynamics. We

attribute this to surface energy effects, the $(MgH_2)_n$ clusters reconstruct from the bulk into lower energy structures with a reduced surface energy. Thus reconstruction enhances their stability compared to the bulk. This phenomenon can be generalised to many hydrogen storage, and indeed gas-storage materials, although the details of whether this will enhance or reduce stability will also depend on the stability of the dehydrided material. Any improvements observed in H_2 release properties by nanostructuring MgH_2 are primarily kinetic, e.g. increasing the specific surface area. We have extrapolated trends in stability from the larger "amorphous" clusters to the bulk. We demonstrated that the amorphous structures do not strongly reduce dehydrogenation enthalpy. Improvements in thermodynamics, if any, are minor. In principle, the smallest "bulk-like" MgH_2 cluster will have a lower dehydrogenation enthalpy than the bulk, however such clusters will be of a size larger than considered in this Paper. It is essential to accurately determine the structures of cluster in order to understand the trends of properties at the nanoscale.

We have also investigated the thermodynamics of transition-metal doping of bulk and nanoparticulate MgH_2. We find that, compared to the bulk, substitutional doping of nanoparticulate MgH_2 is substantially easier. Indeed, $(MgH_2)_{5,6,8,9}$ are all magic numbers for Ni-doping, as they have dopant formation energies that approximately zero or are negative. This is due to the large effective surface areas. Furthermore, we demonstrate that Ni-doping enhances H_2-release thermodynamics, enabling initial H_2 release at substantially lower energies than for the undoped $(MgH_2)_n$ clusters. This is due to the presence of the empty d-states of the Ni dopant modifying the binding and lessening the

charge of H^- ions, weakening the Mg-H bond and allowing lower temperature H_2 release, with major implications for optimising the hydrogen-release properties of MgH_2.

Our calculations thus show that, based on a study of low energy structures, nanostructuring by itself will not allow MgH_2 to function as a near-room-temperature store. However, we also demonstrate that nanostructuring allows facile transition metal doping and that this is a route towards improved hydrogen storage thermodynamics. It is clear that MgH_2 nanostructuring in combination with transition metal doping is a route towards low-temperature hydrogen storage and release. We suggest that designing novel MgH_2 hydrogen storage systems by combining these approaches will result in radically improved dehydrogenation thermodynamics. We therefore urge that further experimental and theoretical investigations be performed on these systems to clarify electronic and structural properties.

Supporting Information

Density Functional Theory lattice parameters of Mg and MgH_2, lowest energy and selected second lowest energy structures of $(MgH_2)_n$ of clusters as obtained using PBE, LDA, PBESol and B3LYP exchange correlation functionals, and tabulated dehydrogenation enthalpies for $(MgH_2)_n$ clusters as obtained with LDA, PBESol and B3LYP exchange correlation functionals. This information is available free of charge via the Internet at http://pubs.acs.org.

Acknowledgements

References

[1] White, C. M.; Steeper, R. R.; and Lutz, A. E.; The hydrogen-fueled internal combustion engine: a technical review. *Int. J. Hydro. Ene.* **2006**, 31, 1292-1305

[2] Schlapbach, L. and Züttel, A.; Hydrogen-storage materials for mobile applications. *Nature* **2001**, 414, 353-359

[3] Bardhan, R.; Rumininski, A. M.; Brand, A.; and Urban, J. J.; Magnesium nanocrystal-polymer composites: A new platform for designer hydrogen storage materials. *Energy Environ. Sci.* **2011**, 4, 4882-4895

[4] Shevlin, S. A.; and Guo, Z. X.; Density functional theory simulations of complex hydride and carbon-based hydrogen storage materials. *Chem. Soc. Rev.* **2009**, 38, 211-226

[5] Lei, Y.; Shevlin, S. A.; Zhu, W.; and Guo, Z. X.; Hydrogen-induced magnetization and tunable hydrogen storage in graphitic structures. *Phys. Rev. B* **2008**, 77, 134114

[6] Aguey-Zinsou, K-F.; and Ares-Fernández, J. R.; Hydrogen in magnesium: new perspectives toward functional stores. *Energy. Environ. Sci.* **2010**, 3, 526-543

[7] Shevlin, S. A.; Cazorla, C.; and Guo, Z. X.; Structure and Defect Chemistry of Low- and High-Temperature Phases of $LiBH_4$. *J. Phys. Chem. C* **2012**, 116, 13488-13496

[8] Shao, H.; Felderhoff, M.; Schüth, F.; and Weidenthaler, C.; Nanostructured Ti-catalyzed MgH_2 for hydrogen storage. *Nanotech.* **2011, 22**, 235401

[9] Bobet, J.-L.; Event, C.; Nakamura, Y.; Akiba, E.; and Darriet, B.; Synthesis of magnesium and titanium hydride via reactive mechanical alloying - Influence of 3d-metal addition on MgH_2 synthesize. *J. Alloys Comp.* **2000**, 298, 279-284

[10] Lu, H. B.; Poh, C. K.; Zhang, L. C.; Guo, Z. P.; Yu, X. B.; and Liu, H. K.; Dehydrogenation characteristics of Ti- and Ni/Ti-catalyzed Mg hydrides. *J. Alloys. Compd.* **2009**, 481, 152-155

[11] Yang, W. N.; Shang, C. X.; and Guo, Z. X.; Site density effect of Ni particles on hydrogen desorption of $MgH_{(2)}$ *Int. J. Hydro. Ene.* **2010**, 35, 4534-4542

[12] Walker, G. S.; Abbas, M.; Grant, D. M.; and Udeh, C.; Destabilisation of magnesium hydride by germanium as a new potential multicomponent hydrogen storage system. *Chem. Comm.* **2011**, 47, 8001-8003

[13] Jeon, K.-J.; Moon, H. R.; Rumininski, A. M.; Jiang, B.; Kisielowski, C.; Bardhan, R.; and Urban, J. J.; Air-stable magnesium nanocomposites provide rapid and high-capacity hydrogen storage without using heavy-metal catalysts. *Nature Mat.* **2011**, 10, 286-290

[14] Harder, S.; Spielmann, J.; Intemann, J.; and Bandmann, H.; Hydrogen Storage in Magnesium Hydride: The Molecular Approach. *Ange. Chemie. Int. Ed.* **2011**, 50, 4156-4160

[15] Aguey-Zinsou, K-F.; and Ares-Fernández, J. R.; Synthesis of colloidal magnesium: A near room emperature store for hydrogen. *Chem. Mater.* **2007**, 20, 376-378

[16] Du, A. J.; Smith, S. C.; and Lu, G. Q.; First-principle studies of the formation and diffusion of hydrogen vacancies in magnesium hydride. *J. Phys. Chem. C* **2007**, 111, 8360-8365

[17] Wagemanns, R. W. P.; van Lenthe, J. H.; de Jongh, P. E.; van Dillen, A. J.; and de Jongh, K. P.; Hydrogen storage in magnesium clusters: Quantum chemical study. *J. Amer. Chem. Soc.* **2005**, 127, 16675-16680

[18] Larsson, P.; Moysés Araújo, C.; Larsson, J. A.; Jena, P.; and Ahuja, R.; Role of catalysts in dehydrogenation of MgH_2 nanoclusters. *Proc. Nat. Acad.* **2008**, 105, 8227-8231

[19] Wu, Z.; Allendorf, M. D.; and Grossman, J. C.; Quantum Monte Carlo Simulation of Nanoscale MgH_2 Cluster Thermodynamics. *J. Amer. Chem. Soc.* **2009**, 131, 13918-13919

[20] Koukaras, E. N.; Zdetsis, A. D.; and Sigalas, M. M.; Ab Initio Study of Magnesium and Magnesium Hydride Nanoclusters and Nanocrystals: Examining Optimal Structures and Compositions for Efficient Hydrogen Storage. *J. Amer. Chem. Soc.* **2012**, 134, 15914-15922

[21] Woodley, S. M.; and Catlow, C. R. A.; Crystal structure prediction from first principles. *Nature Mat.* **2008**, 7, 937-946

[22] Shevlin, S. A.; and Woodley S. M.; Electronic and Optical Properties of Doped and Undoped $(TiO_2)_{(n)}$ Nanoparticles. *J. Phys. Chem. C* **2010**, 114, 17333-17344

[23] Jansen, M.; Pentin, I. V.; and Schon, J. C.; A Universal Representation of the States of Chemical Matter Including Metastable Configurations in Phase Diagrams. *Angew. Chem. Int. Ed.* **2012**, 51, 132-135

[24] Liang, G.; Boily, G. S.; Huot, J.; Van Neste A.; and Schulz, R.; Mechanical alloying and hydrogen absorption properties of the Mg-Ni system. *J. Alloys Comp.* **1998**, 267, 302-306

[25] Song, Y.; Guo, Z. X.; and Yang, R.; Influence of selected alloying elements on the stability of magnesium dihydride for hydrogen storage applications: A first-principles investigation. *Phys. Rev. B.* **2004**, 69, 094205

[26] Chen, D.; Wang, Y. M.; Chen, L.; Liu, S.; Ma, C. X.; and Wang, L. B.; Alloying effects of transition metals on chemical bonding in magnesium hydride MgH_2. *Acta Mat.* **2004**, 52, 521-528

[27] Oelerich, W.; Klassen, T.; and Bormann, R.; Metal oxides as catalysts for improved hydrogen sorption in nanocrystalline Mg-based materials. *J. Alloys Comp.* **2001**, 315, 237-242

[28] Shang, C. X.; and Guo, Z. X.; Effect of carbon on hydrogen desorption and absorption of mechanically milled MgH_2. *J. Power Sour.* **2004**, 129, 73-80

[29] Imamura, H.; Sakasai, N.; and Fujinaga T.; Characterization and hydriding properties of Mg-graphite composites prepared by mechanical grinding as new hydrogen storage materials. *J. Alloys Comp.* **1997**, 253, 34-37

[30] Reule, H.; Hirscher, M.; Weisshardt, A.; and Kronmuller, H.; Hydrogen desorption properties of mechanically alloyed MgH_2 composite materials. *J. Alloys Comp.* **2000**, 305, 246-252

[31] Kresse, G.; Efficiency of ab-initio total energy calculations for metals and semiconductors using a plane-wave basis set. *J. Comp. Mat. Sci.* **1996**, 6, 15-50

[32] Shevlin, S. A.; Fisher, A. J.; and Hernandez, E.; Series of ($n\times2$) Si-rich reconstructions of beta-SiC(001): A prospective atomic wire. *Phys. Rev. B* **2001**, 63, 195306

[33] Blöchl, P.; PROJECTOR AUGMENTED-WAVE METHOD. *Phys. Rev. B* **1994**, 50, 17953

[34] Ceperley, D. M.; and Alder, B. J.; GROUND-STATE OF THE ELECTRON-GAS BY A STOCHASTIC METHOD. *Phys. Rev. Lett.* **1980**, 45, 566-569

[35] Perdew, J. P.; Burke, K.; and Ernzerhof, M.; Generalized gradient approximation made simple. *Phys. Rev. Lett.* **1996**, 77, 3865-3868

[36] Perdew, J. P.; Ruzsinszky, A.; Csonka, G. I.; Vydrov, O. A.; Scuseria, G. E.; Constantin, L. A.; Zhou, X.; and Burke, K.; Restoring the density-gradient expansion for exchange in solids and surfaces. *Phys. Rev. Lett.* **2008**, 100, 136406

[37] Becke, A. D.; Density-functional thermochemistry .4. A new dynamical correlation functional and implications for exact-exchange mixing. *J Chem. Phys.*, 1996, **104**, 1040

[38] Lee, C.; Yang, W.; and Parr, R. G.; DEVELOPMENT OF THE COLLE-SALVETTI CORRELATION-ENERGY FORMULA INTO A FUNCTIONAL OF THE ELECTRON-DENSITY. *Phys. Rev. B*, 1988, **37**, 785

[39] Janacek, S.; Krotscheck, E.; Liebrecht, M.; and Wahl, R.; Structure of Mg_n and Mg_n^+ clusters up to n=30. *Eur. Phys. J. D*, **2011**, 63, 377-391

[40] Shevlin, S. A.; Kerkeni, B.; and Guo, Z. X.;Dehydrogenation mechanisms and thermodynamics of MNH_2BH_3 (M = Li, Na) metal amidoboranes as predicted from first principles. *Phys. Chem. Chem. Phys.* **2011**, 13, 7649-7660

[41] Bortz, M.; Bertheville, B.; Bottger, G.; and Yvon, K.; Structure of the high pressure phase gamma-MgH_2 by neutron powder diffraction. *J. Alloys. Comp.* **1999**, 287, L4-L6

[42] Qu, Z.-W.; and Kroes, G.-J.; Theoretical study of the electronic structure and stability of titanium dioxide clusters $(TiO_2)(n)$ with n=1-9. *J. Phys. Chem. B* **2006**, 110, 8998-9007

[43] Catalyud, M.; Maldonado, L.; and Minot, C.; Reactivity of $(TiO_2)(N)$ Clusters (N=1-10): Probing Gas-Phase Acidity and Basicity Properties. *J. Phys. Chem. C* **2008**, 112, 16087-16095

[44] Li, S.; and Dixon, D. A.; Molecular structures and energetics of the $(TiO_2)(n)$ (n=1-4) clusters and their anions. *J. Phys. Chem. A*, **2008**, 112, 6646-6666

[45] Marom, N.; Kim, M.; and Chelikowsky, J. R.; Structure Selection Based on High Vertical Electron Affinity for TiO_2 Clusters. *Phys. Rev. Lett.* **2012**, 108, 106801

[46] Flikkema, E.; and Bromley, S. T.; Dedicated global optimization search for ground state silica nanoclusters: $(SiO_2)(N)$ (N=6-12). *J. Phys. Chem. B* **2004**, 108, 9638-9645

[47] Francisco, E.; Martin Pendas, A.; and. Blanco, M. A.; Global optimization of ionic Mg_nF_{2n} (n=1-30) clusters. *J. Chem. Phys.* **2005**, 123, 234305

[48] Neelaramju, S.; Bach, A.; Schön, J. C.; Fischer, D.; and Jansen, M.; Experimental and theoretical study on Raman spectra of magnesium fluoride clusters and solids. *J. Chem. Phys.* **2012**, 137, 194319

[49] Pozzo, M.; and Alfè, D.; Structural properties and enthalpy of formation of magnesium hydride from quantum Monte Carlo calculations. *Phys. Rev. B* **2008**, 77, 104103

[50] Norberg, N. S.; Arthur, T. S.; Fredrick, S. J.; and Prieto, A. L.; Size-Dependent Hydrogen Storage Properties of Mg Nanocrystals Prepared from Solution. *J. Amer. Chem. Soc.* **2011**, 133, 10679-10681

[51] Reich, J. M.; Wang, L.-L.; and Johnson, D. D.; Surface and Particle-Size Effects on Hydrogen Desorption from Catalyst-Doped MgH$_2$. *J. Phys. Chem. C* **2012**, 116, 20315-20320

[52] Kim, K. C.; Dai, B.; Johnson, J. K.; and Sholl, D. S.; Assessing nanoparticle size effects on metal hydride thermodynamics using the Wulff construction. *Nanotech.* **2009**, 20, 204001

[53] Li, L.; Peng, B.; Ji, W.; and Chen, J.; Studies on the Hydrogen Storage of Magnesium Nanowires by Density Functional Theory. *J. Phys. Chem. C* **2009** 113, 3007-3013

[54] S. Hao, S.; and Sholl, D. S.; Selection of dopants to enhance hydrogen diffusion rates in MgH$_2$ and NaMgH$_3$. *Appl. Phys. Lett.* **2009**, 94, 171909
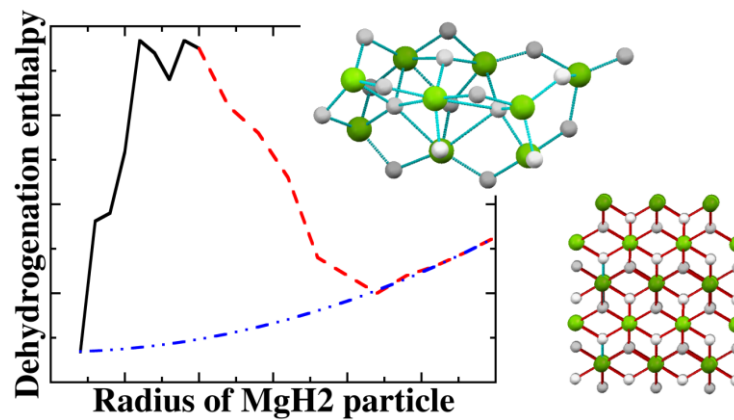
The structures and thermodynamics of bare and Ni-doped $(MgH_2)_n$ nanoparticles were determined by *ab initio* simulation. In contrast to predictions from classical theory (blue line), dehydrogenation enthalpy increases with decreasing nanoparticle size (black line) for majority of nanoparticle sizes. This is due to radically different nanoparticle structures with respect to the bulk. For larger nanoparticle sizes, we predict there will be convergence to dehydrogenation enthalpies that are not radically different from the bulk (red line).